Available online at www.sciencedirect.com
SCIENCE DIRECT®
C. R. Physique 5 (2004) 315–324
COMPTES RENDUS PHYSIQUE

Highly polarized nuclear spin systems and dipolar interactions in NMR/Systèmes de spins nucléaires fortement polarisés et interactions dipolaires en RMN

Transfer of para-hydrogen spin order into polarization by diabatic field cycling

Haukur Jóhannesson *, Oskar Axelsson, Magnus Karlsson

Amersham Health R&D AB, Medeon, 205 12 Malmö, Sweden

Available online 17 April 2004

Presented by Guy Laval

Abstract

In a para-hydrogen induced polarization (PHIP) experiment, it is possible to obtain a substantial net polarization of a hetero nucleus using a diabatic field cycling scheme. This is experimentally demonstrated for hydroxyethyl propionate. The screening of the ambient magnetic field was accomplished by using several concentric mu-metal cylinders. The field cycling is modeled as a sudden decrease from intermediate field to low field, followed by an adiabatic remagnetization. An analytical expression for the polarization as a function of the constituent scalar couplings, using an idealized field cycling profile, is derived for an AA′X spin system. It is also demonstrated that the hyperpolarized compound can be used for magnetic resonance imaging (MRI). ***To cite this article: H. Jóhannesson et al., C. R. Physique 5 (2004).***

Résumé

Transfert de cohérence de spin de para hydrogène à polarisation par changement diabatique du champ magnétique. Dans une expérience de polarisation induite par para hydrogène (PHIP), il est possible d'obtenir une polarisation substantielle sur un hétéronoyau par l'utilisation d'une technique de changement diabatique du champ magnétique. Cela est démontré expérimentalement dans le cas du propionate d'hydroxyethyle. Le champ ambiant est réduit avec plusieurs cylindres concentriques de mu-métal. La variation du champ magnétique est modélisée comme une transition abrupte d'un champ intermédiaire vers un champ très faible suivie par une réaimantation adiabatique. Une expression analytique de la polarisation en fonction des couplages scalaires est dérivée pour un système de spins AA′X en considérant un profil de champ magnétique idéalisé. Il est aussi démontré que l'entitée hyperpolarisée peut être utilisée pour l'imagerie par résonance magnétique (IRM). ***Pour citer cet article : H. Jóhannesson et al., C. R. Physique 5 (2004).***

Keywords: Para-hydrogen induced polarization; Diabatic; Field cycling

Mots-clés : Polarisation induite par para hydrogène ; diabatique ; champ magnétique cyclé

1. Introduction

The para-hydrogen induced polarization (PHIP) discovered by Bowers and Weitekamp in 1986 [1,2] has provided a powerful tool for investigating catalytic processes. The PHIP phenomenon was initially divided into two seemingly different categories, PASADENA [2] and ALTADENA [3], depending on whether the applied field during hydrogenation was high or low. The early

* Corresponding author.
E-mail address: haukur.johannesson@amersham.com (H. Jóhannesson).

1631-0705/$ – see front matter
doi:10.1016/j.crhy.2004.02.001

simplistic interpretations assuming slow or rapid breaking of the symmetry of the singlet state of para-hydrogen [3,4] did not provide a satisfactory explanation for the differences between the PASADENA and ALTADENA phenomena, nor did they allow a smooth transition between the two cases. A more rigorous approach is to use the density operator formalism to describe the PHIP phenomenon.

Spontaneous transfer of spin order from the protons to a hetero nucleus has been subject to extensive studies. Initial work in this field attributed the presence of enhanced NMR signals for hetero nuclei to dipolar relaxation [5,6], but later it was shown, both experimentally and by density operator calculations, that it is usually not necessary to include relaxation in order to explain the occurrence of enhanced hetero nuclei signals [7,8]. Several pulse sequences, most of them based on the INEPT sequence, have been developed to transfer spin order from protons to hetero nuclei [9,10]. An early study using PHIP for magnetic resonance imaging (MRI) has been published from our lab [11]. A review on the PHIP phenomenon has been written by Bowers [12].

The outline of the present paper is as follows: in Section 2 we give a short description of the origin of the PHIP effect. In Section 3 we consider an AA′X system and obtain the spin density operator for a spin system that has been hydrogenated with para-hydrogen. An analytical expression for the polarization of a hetero nucleus that has been subject to diabatic–adiabatic field cycling is obtained in Section 4. In Section 5 the expression for the carbon polarization is compared to numerical simulations, and deviations from the idealized field cycling are discussed. The experimental results are finally described in Section 6.

2. Properties of para-hydrogen

The PHIP phenomenon is explained from the quantum statistical mechanical properties of homonuclear diatomic molecules. From quantum mechanical symmetry requirements the total wave function for di-hydrogen must be anti-symmetric with respect to exchange of the two protons [13]. It then follows that the symmetric nuclear states (ortho-hydrogen) are correlated to anti-symmetric rotational states with odd rotational quantum numbers, and that the anti-symmetric nuclear state (para-hydrogen) is correlated to symmetric rotational states with even rotational quantum numbers [14].

The anti-symmetric nuclear spin state is given by $|\psi^P\rangle = \frac{1}{\sqrt{2}}(|\alpha\beta\rangle - |\beta\alpha\rangle)$, and the three symmetric states by $|\psi_1^0\rangle = |\alpha\alpha\rangle$, $|\psi_2^0\rangle = |\beta\beta\rangle$, $|\psi_3^0\rangle = \frac{1}{\sqrt{2}}(|\alpha\beta\rangle + |\beta\alpha\rangle)$.

The fraction of para-hydrogen in hydrogen gas at thermal equilibrium is

$$x_p \equiv \frac{N_{\text{para}}}{N_{\text{ortho}} + N_{\text{para}}} = \frac{\sum_{J\text{even}} (2J+1)\, \mathrm{e}^{-\Theta_r J(J+1)/T}}{\sum_{J\text{even}} (2J+1)\, \mathrm{e}^{-\Theta_r J(J+1)/T} + 3\sum_{J\text{odd}} (2J+1)\, \mathrm{e}^{-\Theta_r J(J+1)/T}},$$

where $\Theta_r = \hbar^2/(2k_B I)$ is the so-called characteristic temperature of rotation, being equal to $\Theta_r \sim 85.3$ K for di-hydrogen [14]. In the high temperature limit ($T \to \infty$) this ratio is equal to $1/4$, but for $T = 0$ we have 100% para-hydrogen. At low temperatures di-hydrogen is in its lowest rotational state ($J = 0$) and does not rotate. The temperature dependence of x_p is plotted in Fig. 1.

The spin density operators of para- and ortho-hydrogen are given by $\sigma_{\text{para}} = \frac{1}{4}(\mathbf{1} - 4\hat{\mathbf{I}}_1 \cdot \hat{\mathbf{I}}_2)$ and $\sigma_{\text{ortho}} = \frac{1}{4}(\mathbf{1} + \frac{4}{3}\hat{\mathbf{I}}_1 \cdot \hat{\mathbf{I}}_2)$ respectively. For a mixture of the two spin isomers with a molar fraction of para-hydrogen given by x_p, the total spin density operator is $\sigma_{\text{H}_2} = x_p\sigma_{\text{para}} + (1 - x_p)\sigma_{\text{ortho}} = \frac{1}{4}(\mathbf{1} - f\hat{\mathbf{I}}_1 \cdot \hat{\mathbf{I}}_2)$, with $f = \frac{4}{3}(4x_p - 1)$.

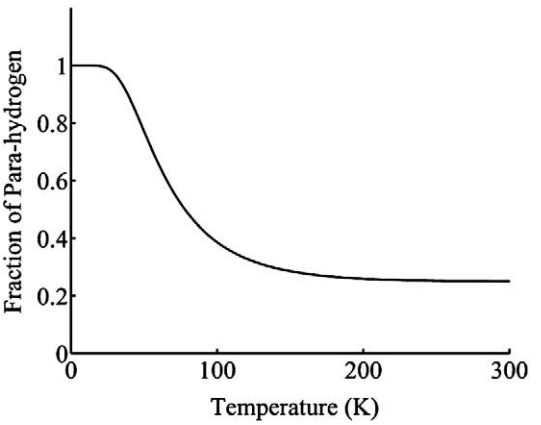

Fig. 1. Equilibrium fraction of para-hydrogen as a function of temperature.

3. Hydrogenation with para-hydrogen

3.1. Introduction

Consider a molecule containing N nuclei with spin $s \neq 0$ being hydrogenated with para-hydrogen. The resulting spin density operator for the total spin system is initially given by $\sigma_{\text{tot}} = \sigma_{\text{H}_2} \otimes \sigma_N$, where σ_N is the spin density operator describing the spin system of the molecule prior to hydrogenation. Using hydrogen gas enriched in the para (or ortho) isomer, and assuming high temperature condition for the density operator σ_N, we can approximate $\sigma_N = \frac{1}{\text{tr}(\mathbf{1})}\mathbf{1}$, where $\text{tr}(\mathbf{1})$ is the dimension of the Hilbert space of the N spin system. The total spin density operator is then given by

$$\frac{1}{\text{tr}(\mathbf{1})}(\mathbf{1} - f\hat{\mathbf{I}}_1 \cdot \hat{\mathbf{I}}_2), \tag{1}$$

where now $\text{tr}(\mathbf{1})$ is the dimension of the total Hilbert space of the $N + 2$ spin system.

During the hydrogenation process, the spin systems of different molecules will start their evolution in the ambient magnetic field under the influence of the corresponding Hamiltonian. This means that if the hydrogenation of the molecules in the sample is spread out in time, we will have a distribution of states that have started their evolution at different times. The final spin density operator of the system after hydrogenation must be taken as the ensemble average of the different spin density operators. If the reaction time is long compared to the inverse scalar couplings of the system, all off-diagonal terms in the eigenbase of the Hamiltonian will vanish upon averaging. Since any expectation value, e.g., the magnetization, involves the trace of the product of the density matrix and a spin operator, the signal intensity will be proportional to the constant f since it factors out of the trace. This implies that we without loss of generality can assume that $x_p = 1$, i.e., that we have 100% para-hydrogen.

3.2. The three spin system

The derivation of the ^{13}C polarization, following a diabatic–adiabatic field cycling requires the eigenstates of the Hamiltonian at the initial and final field strengths. We solve this problem analytically for a three-spin system consisting of the two protons originating from para-hydrogen and a ^{13}C nucleus. We obtain an equation for the carbon polarization involving coefficients of the eigenstates at the initial and final field strengths of the field cycling. In the following, the indices 1 and 2 refer to the protons and the index 3 to the carbon nucleus, and the indices of product states, $|ijk\rangle$, are enumerated from left to right.

The Hamiltonian for the relevant spin–spin interactions is given by

$$H = -\omega_{H,1} I_{1z} - \omega_{H,2} I_{2z} - \omega_C I_{3z} + 2\pi \sum_{i,j} J_{ij} \hat{\mathbf{I}}_i \cdot \hat{\mathbf{I}}_j. \tag{2}$$

Depending on the applied external magnetic field strength we can distinguish three different regimes where the Hamiltonian takes a simpler form.

$$\text{(i)} \quad \omega_i \ll J_{jk} \quad \forall i, j, k, \tag{3a}$$

$$\text{(ii)} \quad |\omega_{H,1} - \omega_{H,2}| \ll J_{jk} \ll \omega_{H,i} - \omega_C \quad \forall i, j, k, \tag{3b}$$

$$\text{(iii)} \quad J_{ij} \ll |\omega_{H,1} - \omega_{H,2}| \quad \forall i, j. \tag{3c}$$

Expressed in NMR jargon these cases correspond to AA′A″, AA′X and ABX spin systems respectively. In what follows the corresponding field strengths will be referred to as being low, intermediate and high respectively. For the initial field strength used during hydrogenation, which is of the order of 0.1 mT, we have an AA′X system, and for the lowest field strength of the field cycling we have an AA′A″ spin system.

3.3. Eigenstates at intermediate field strength

At intermediate field, the Hamiltonian is given by

$$H = -\omega_H(I_{1z} + I_{2z}) - \omega_C I_{3z} + 2\pi(J_{12}\hat{\mathbf{I}}_1 \cdot \hat{\mathbf{I}}_2 + J_{13} I_{1z} \cdot I_{3z} + J_{23} I_{2z} \cdot I_{3z}).$$

The Hamiltonian is block-diagonal with two 2×2 subspaces (corresponding to the carbon spin states $s = \pm 1/2$) each of which can easily be diagonalized. The eigenvalues of the two 2×2 matrices are given by $E_{1\pm} = -\frac{\omega_C}{2} - \frac{\pi J_{12}}{2} \pm \pi\Omega$ and $E_{2\pm} = \frac{\omega_C}{2} - \frac{\pi J_{12}}{2} \pm \pi\Omega$, where $\Omega = \sqrt{\Delta^2 + J_{12}^2}$, and $\Delta = (J_{23} - J_{13})/2$. The corresponding eigenstates (up to an arbitrary phase) are

$$\Psi_{1\pm} = c_\pm|\alpha\beta\alpha\rangle \mp c_\mp|\beta\alpha\alpha\rangle, \tag{4a}$$

$$\Psi_{2\pm} = c_{\mp}|\alpha\beta\beta\rangle \mp c_{\pm}|\beta\alpha\beta\rangle, \tag{4b}$$

where $c_{\pm} = q_{\pm}/\sqrt{(1+q_{\pm}^2)}$, and $q_{\pm} = (\Delta \mp \Omega)/J_{12}$.

3.4. Eigenstates at zero field strength

At zero field, the Hamiltonian is given by $H = 2\pi \sum_{i,j} J_{ij}\hat{\mathbf{I}}_i \cdot \hat{\mathbf{I}}_j$. It is block-diagonal with two 3×3 subspaces (corresponding to a total spin $S = \pm 1/2$ for all three spins). The eigenvalues are the same for both 3×3 matrices and are given by $E'_0 = \frac{\pi\Sigma}{2}$, where $\Sigma = J_{12}+J_{13}+J_{23}$ and $E'_{\pm} = -\frac{\pi\Sigma}{2} \pm \pi\Lambda$, where $\Lambda = \sqrt{\Sigma^2 - 3\Gamma^2}$, and $\Gamma^2 = J_{12}J_{13} + J_{12}J_{23} + J_{13}J_{23}$. The corresponding eigenstates are (up to an arbitrary phase)

$$\Phi_{1,0} = \frac{1}{\sqrt{3}}|\alpha\alpha\beta\rangle + \frac{1}{\sqrt{3}}|\alpha\beta\alpha\rangle + \frac{1}{\sqrt{3}}|\beta\alpha\alpha\rangle, \tag{5a}$$

$$\Phi_{1\pm} = c_1^{\pm}|\alpha\alpha\beta\rangle + c_2^{\pm}|\alpha\beta\alpha\rangle + c_3^{\pm}|\beta\alpha\alpha\rangle, \tag{5b}$$

$$\Phi_{2,0} = \frac{1}{\sqrt{3}}|\alpha\beta\beta\rangle + \frac{1}{\sqrt{3}}|\beta\alpha\beta\rangle + \frac{1}{\sqrt{3}}|\beta\beta\alpha\rangle, \tag{5c}$$

$$\Phi_{2\pm} = \mp c_3^{\pm}|\alpha\beta\beta\rangle + \mp c_2^{\pm}|\beta\alpha\beta\rangle + \mp c_1^{\pm}|\beta\beta\alpha\rangle, \tag{5d}$$

where

$$c_1^{\pm} = -(J_{12} - J_{23} \pm \Lambda)/\Theta^{\pm}, \quad c_2^{\pm} = -(J_{23} - J_{13} \mp \Lambda)/\Theta^{\pm}, \quad c_3^{\pm} = (J_{12} - J_{13})/\Theta^{\pm}, \quad \text{and}$$
$$\Theta^{\pm} = \sqrt{(J_{12} - J_{13})^2 + (J_{12} - J_{23} \pm \Lambda)^2 + (J_{23} - J_{13} \mp \Lambda)^2}.$$

The remaining two eigenstates $|\alpha\alpha\alpha\rangle$ and $|\beta\beta\beta\rangle$ both have the eigenvalues $\pi\Sigma/2$. Thus there are two pairs of doubly degenerate levels as well as four quadruply degenerate levels.

3.5. The averaged density operator

After hydrogenation with para-hydrogen, the initial spin density operator is given by the projection of the operator $\sigma = \frac{1}{\mathrm{tr}(\mathbf{1})}(\mathbf{1} - 4\hat{\mathbf{I}}_1\hat{\mathbf{I}}_2)$ on the eigenstates of the Hamiltonian. This averaging of the off-diagonal elements will produce a diagonal density matrix in the eigenbase of the Hamiltonian. For the high field case, the eigenstates are the simple product functions and the only term that survives in the scalar product contains the z-components, leading to the averaged density operator $\bar{\sigma} = \frac{1}{8}(\mathbf{1} - 4I_{1z}I_{2z})$. For the intermediate field, the eigenstates are $|\alpha\alpha\alpha\rangle$, $|\alpha\alpha\beta\rangle$, $|\Psi_{1-}\rangle$, $|\Psi_{1+}\rangle$, $|\Psi_{2-}\rangle$, $|\Psi_{2+}\rangle$, $|\beta\beta\alpha\rangle$, $|\beta\beta\beta\rangle$, and the averaged spin density operator is given by [8] $\bar{\sigma} = \frac{1}{8}(\mathbf{1} - 4(I_{1z}I_{2z} + \Gamma))$ where $\Gamma = \frac{1}{1+\eta^2}(I_{1x}I_{2x} + I_{1y}I_{2y}) + \frac{\eta}{1+\eta^2}(I_{1z} - I_{2z})I_{3z}$ with $\eta = \Delta/J_{12}$. The only non-zero elements of the averaged density matrix, $\bar{\sigma}$, are the four diagonal elements

$$\langle\Psi_{1-}|\bar{\sigma}|\Psi_{1-}\rangle = \langle\Psi_{2-}|\bar{\sigma}|\Psi_{2-}\rangle = \frac{1}{4}(c_- - c_+)^2$$

and

$$\langle\Psi_{1+}|\bar{\sigma}|\Psi_{1+}\rangle = \langle\Psi_{2+}|\bar{\sigma}|\Psi_{2+}\rangle = \frac{1}{4}(c_- + c_+)^2,$$

representing the populations of the four eigenstates. For an AA′X spin system the initial populations of the eigenstates after hydrogenation with para-hydrogen are thus solely determined by the scalar couplings of the system.

4. Diabatic field cycling

After the diabatic transfer to zero field the elements of the density matrix, using the initial base, are unchanged whereas the density matrix in the eigenbase of the Hamiltonian H_J has changed according to $T^{-1}\bar{\sigma}T$, where the columns of T are the eigenstates of the zero-field Hamiltonian expressed in the eigenbase of the intermediate-field Hamiltonian. For calculational purposes it is convenient to decompose T as $T = T_i^{-1}T_z$, where T_i and T_z denote the transformation matrices from the base of product functions to the eigenbase of the intermediate and zero field Hamiltonians respectively. The columns of T_i and T_z are given by the eigenvectors in Eqs. (4) and (5) respectively.

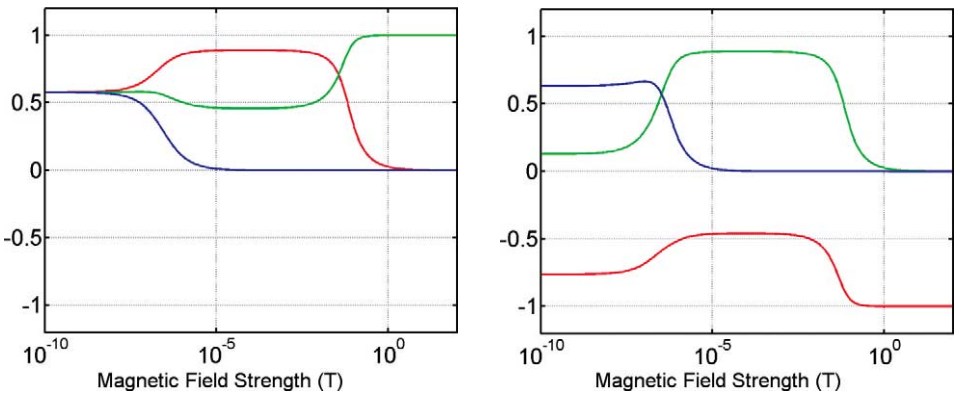

Fig. 2. Field dependence of two of the eigenstates for some typical values of the couplings. The figure shows the coefficients of a general superposition $c_1|\alpha\alpha\beta\rangle + c_2|\alpha\beta\alpha\rangle + c_3|\beta\alpha\alpha\rangle$ for the transitions $\Phi_{1,0} \rightarrow \Psi_{1+}$ (left) and $\Phi_{1+} \rightarrow \Psi_{1-}$ (right). The colors blue, green, and red refer to the coefficients c_1, c_2, and c_3 respectively.

The adiabatic transfer from low field to intermediate field leaves the populations of the instantaneous Hamiltonian unchanged. As the field increases, the eigenstates at zero field continuously change to the eigenstates of the intermediate field: $|\phi\rangle_{\text{low field}} \rightarrow |\phi\rangle_{\text{intermediate field}}$. The eigenvalues and eigenstates can be calculated for an arbitrary field by numerical methods allowing one to monitor the continuous transformation between the low and intermediate field states. Since the eigenstates are orthogonal at all fields there are no avoided crossings of the eigenvalues. The following correlations between the zero and intermediate field states for our spin system were found from numerical calculations: $\Phi_{1,0} \rightarrow \Psi_{1+}$, $\Phi_{1+} \rightarrow \Psi_{1-}$, $\Phi_{1-} \rightarrow |\alpha\alpha\beta\rangle$ and $\Phi_{2,0} \rightarrow |\beta\beta\alpha\rangle$, $\Phi_{2+} \rightarrow \Psi_{2+}$, $\Phi_{2-} \rightarrow \Psi_{2-}$ (see Fig. 2). In the following we assume positive scalar couplings and that this correlation is valid. The validity of this assumption will be manifested in the agreement with the simulation data presented in Section 5.

The carbon polarization after the diabatic–adiabatic process is given by $pol = 2 \cdot \text{tr}(I_{3z}\sigma)$. Carrying out the arithmetic calculations,[1] one arrives at:

$$\begin{aligned} pol = \Big\{ & \frac{1}{2}\big(c_+^4 + c_-^4\big)\big(c_3^- c_2^+ - c_1^- c_3^+ + c_1^- c_2^+ - c_2^- c_3^+\big) \\ & + \big(c_-^3 c_+ - c_+^3 c_-\big)\big(c_1^- c_2^+ - 2c_1^+ c_2^- + c_1^- c_3^+ + c_2^- c_3^+ - 2c_1^+ c_3^- + c_3^- c_2^+\big) \\ & + c_-^2 c_+^2\big(2c_3^- c_3^+ - c_2^- c_3^+ + c_1^- c_3^+ - 2c_2^- c_2^+ + c_3^- c_2^+ - c_1^- c_2^+ + 4c_1^+ c_2^- - 4c_1^+ c_3^-\big)\Big\} \\ & \times\big(c_1^- c_2^+ - c_1^+ c_2^- + c_2^- c_3^+ - c_3^- c_2^+ + c_1^+ c_3^- - c_1^- c_3^+\big)^{-1}. \end{aligned} \tag{6}$$

If the spin system is completely symmetrical, i.e., $\Delta = 0$, there will be no net polarization for the carbon. Eq. (6) correctly predicts zero carbon polarization for $\Delta = 0$ only when the proton–carbon scalar coupling is larger than the proton–proton coupling ($J_{13} = J_{23} > J_{12}$) as can be seen in Fig. 3. When the proton–carbon scalar coupling is smaller than the proton–proton coupling, Eq. (6) fails to give the correct result when $J_{13} = J_{23}$. To include this effect the equation should be multiplied by the factor $1 - \delta_{J_{13}J_{23}}$, where δ_{ij} is the Kronecker delta function, being equal to one if $i = j$ and zero otherwise. This may seem unphysical, but the origin of this singularity is that the adiabatic constraint is not possible to satisfy under these conditions, and the constraint of adiabatic remagnetization thus becomes unphysical. This will be demonstrated in the next section.

5. Simulations

The diabatic–adiabatic field cycling was simulated using a full treatment of the spin–spin interactions, i.e., using Eq. (2). The coupling between the spin system and the lattice, i.e. relaxation, was, however, not considered.

The averaged spin density matrix $\bar{\sigma}$, was obtained by transforming the initial density matrix to the eigenbase of the Hamiltonian at the intermediate field, and subsequently setting all off-diagonal elements to zero. The evolution of the density matrix is given by the Liouville–von Neumann equation, $\dot{\sigma} = -\text{i}[H, \sigma]$, with the formal solution $\sigma(t) = U(t)\sigma(0)U(t)^{-1}$

[1] Since the arithmetic is rather cumbersome the calculations were performed with the assistance of the analytical computation program Maple® 6.

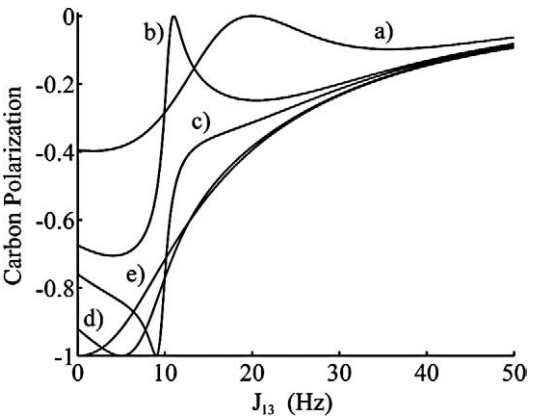

Fig. 3. The carbon polarization according to Eq. (6) as a function of J_{13} for five different values of J_{23}: (a) 20 Hz; (b) 11 Hz; (c) 9 Hz; (d) 5 Hz; and (e) 0 Hz. The proton–proton scalar coupling J_{12} has been fixed to 10 Hz.

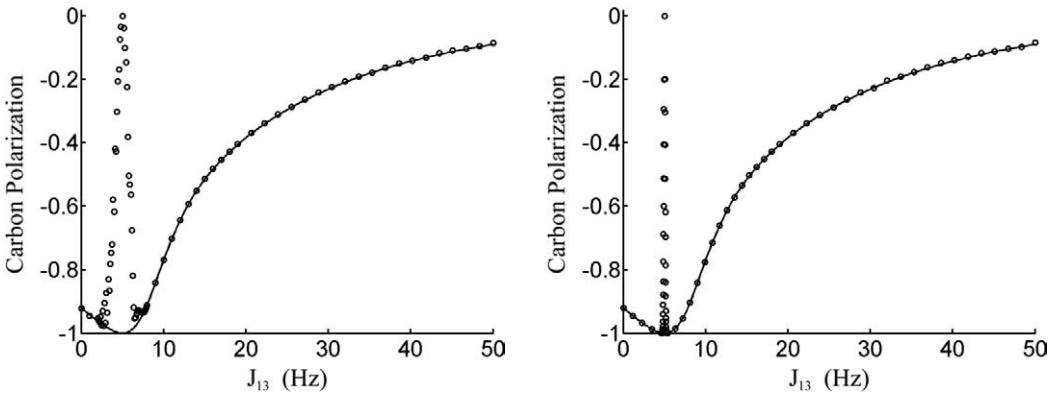

Fig. 4. Carbon polarization as a function of J_{13} obtained from simulation using $J_{23} = 5$ Hz and $J_{12} = 10$ Hz. The remagnetization was done in (a) 10^4 steps with total time duration of 10 s; and (b) 10^5 steps with total time duration of 1000 s. Oscillations in the peak around $J_{13} = 5$ can be seen in the simulation data. The solid line is obtained from Eq. (6).

where $U(t)$ is the time evolution operator. Since the Hamiltonians at different times do not commute, the varying external magnetic field was approximated by a piecewise constant function. This corresponds to an approximation of the Hamiltonian with a piecewise constant operator. Assuming that the magnetic field changes from one discrete value to another at the times $t_1, t_2, \ldots, t_n$ ($t_i < t_j$ when $i < j$), the general expression for the time evolution operator can be written as $U(t) = \exp(-\mathrm{i}H_n\Delta t_n)\cdots\exp(-\mathrm{i}H_1\Delta t_1)$, where $\Delta t_i = t_i - t_{i-1}$ ($t_0 = 0$) and $t = \sum_{j=1}^{n}\Delta t_j$. From a numerical point of view the number of steps in the simulation is primarily determined by the ability to do a smooth sampling of the eigenfunction as it changes between the different regions of Eqs. (3(a)–3(c)) (see Fig. 2). We used the simple approach to increase the time steps exponentially, which was found to give a reasonably rapid convergence.

To test the simulation procedure, the AA′X system was simulated using parameters that as closely as possible resemble the constraints of the analytical calculations. The averaging of the SDO (i.e., the hydrogenation) was performed at 0.1 mT, safely within the intermediate-field region of the spin system, and the zero-field was approximated by 10^{-10} T where we effectively have an AA′A″ spin system (see Fig. 2). The transition to low field was done abruptly in one step, and the remagnetization was performed in 10^4–10^5 steps. Simulation data corresponding to graphs (a) and (b) in Fig. 3 are in agreement with the analytical results (data not shown).

Returning to the issue of the discontinuity of Eq. (6), the simulations show clearly what happens when $J_{13} \approx J_{23} < J_{12}$. The simulations correctly predict zero carbon polarization when the two proton–carbon scalar couplings are equal. Far away from the discontinuity the simulated data converge to the analytical result. The width of the region where the analytic and simulation data disagree depends on how fast the remagnetization is performed, reflecting the problem of satisfying the adiabatic condition (see Fig. 4). When the difference $J_{23} - J_{13}$ is reduced, the derivative of the coefficients of the eigenstates with respect to the

field is increased. This rapid change of the eigenstates within a narrow field interval puts serious constraints on how fast the interval can be traversed, still satisfying the adiabaticity condition. Since the Larmor frequency in this region is only of the order of the size of the scalar couplings, i.e., a few Hertz, the speed at which the field is increased is critical.

At first it may seem somewhat puzzling that when starting with a spin system of essentially zero polarization for both proton and carbon, we can end up with a polarization of the order of unity after a simple field cycling treatment. The explanation has to do with both the initial order (low entropy) of the spin system and the asymetric evolution of different states during remagnetization. Immediately prior to the rapid demagnetization, the individual spin systems are in either of the two superpositions $p_1|\alpha\beta\alpha\rangle + p_2|\beta\alpha\alpha\rangle$ or $q_1|\alpha\beta\beta\rangle + q_2|\beta\alpha\beta\rangle$ where p_i and q_i oscillate in time. At low field these states are not eigenstates of the Hamiltonian and we will have an evolving admixture of these states with $|\alpha\alpha\beta\rangle$ and $|\beta\beta\alpha\rangle$ respectively. At zero field strength the evolution of these states is symmetric, but during the remagnetization the symmetry is broken due to the increasing strength of the Zeeman term of the Hamiltonian. For certain combinations of the scalar couplings the evolution during the remagnetization will favor the contribution of $|\alpha\alpha\beta\rangle$ and at the same time suppress the evolution of $|\beta\beta\alpha\rangle$. This also suggests that a further improvement of the polarization is possible when deviating from the pure adiabatic remagnetization. This will, however, require a remagnetization profile that is optimized individually for each spin system.

The idealized conditions for the diabatic–adiabatic field cycling presented above are hard to realize under realistic experimental conditions. A potential problem might be to obtain a sufficiently low field in the field cycling. From simulations we found that the low field should in general be below 100 nT, and that the transition time should not exceed 1 ms. Another deviation from the idealized field cycling arises from the aforementioned violation of the adiabatic remagnetization. If the required remagnetization time is longer than or comparable with the longitudinal relaxation time a compromize has to be made. In this case an optimized non-adiabatic remagnetization could be an option. The spin system of most relevant organic molecules is in general not a three spin system. Additional protons with non-negligible scalar couplings to the pure three spin system will lead to the evolution of a large number of states and will thus reduce the final polarization of the carbon spins. A simulation of the full spin system of hydroxyethyl propionate, neglecting relaxation, and using realistic field cycling parameters, resembling the experimental conditions outlined in the next section, gives a polarization equal to -28%.

6. Experimental results

Para-hydrogen was produced by passing hydrogen gas through a commercially available catalyst (C*CHEM, P.O. Box 640, Lafayette; Colorado, 80026) at a temperature of 14 K. The para-hydrogen content obtained was found to be better than 95% by NMR. The apparatus for the field cycling experiments is outlined in Fig. 5. The process is under computer control and all liquid

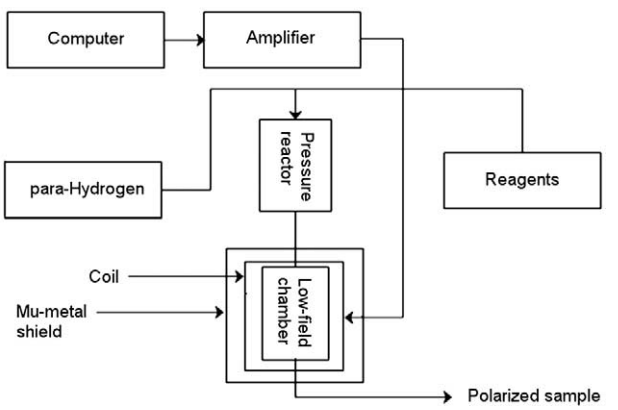

Fig. 5. Schematic representation of the field cycling experiment.

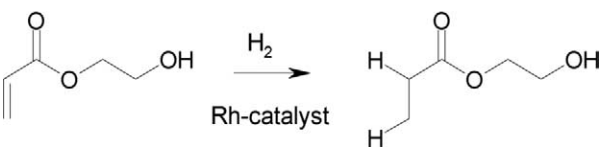

Fig. 6. Chemical reaction of hydrogenation with para-hydrogen. On the left we have hydroxyethyl acrylate, and on the right hydroxyethyl propionate.

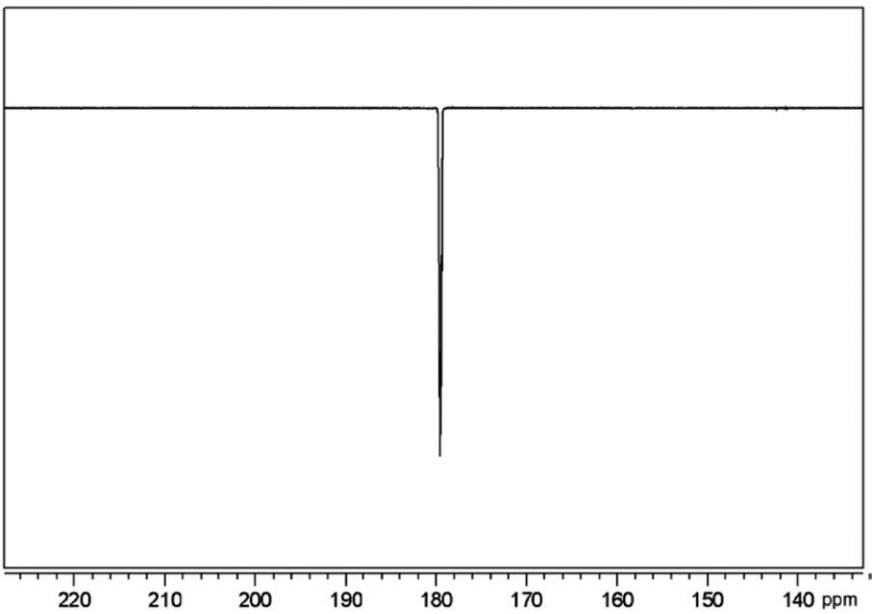

Fig. 7. Carbon spectrum of hydroxyethyl propionate obtained after hydrogenation with para-hydrogen and subsequent field-cycling. The ^{13}C polarization is −21%.

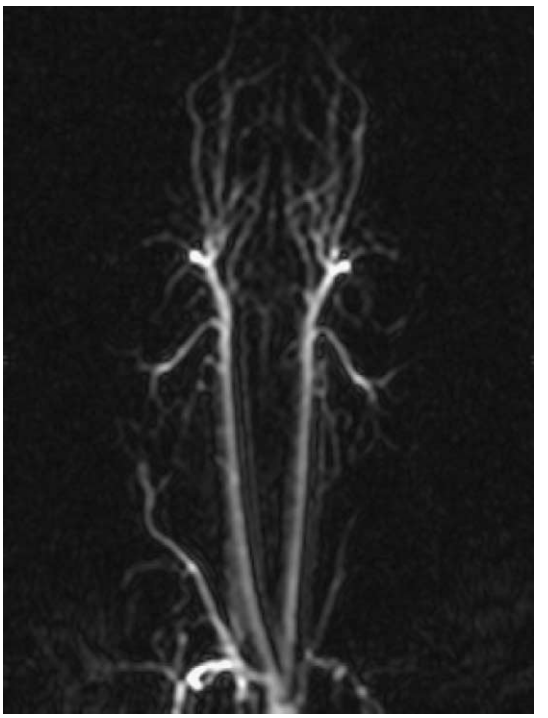

Fig. 8. A ^{13}C angiogram, using the true FISP sequence, showing the head-neck area of a guinea pig.

and gas flows are controlled by solenoid valves. The control software was written in Labview. The process works as follows: A reactor chamber is filled with para-hydrogen to a pressure of 10 bar. The reactors temperature is kept at 333 K, an empirically optimized temperature with respect to the final ^{13}C polarization. A mixture of the substrate and the catalyst is dispensed into the reactor as a narrow jet. After three seconds, the liquid is transferred into the low field chamber with the field initially set

to 100 μT. After a delay of 0.5 s the field is taken down to about 30 nT in 1 ms. The field is then ramped up exponentially to 100 μT according to the desired time constant, whereupon the sample is ejected and collected in a syringe.

The low field chamber is a small glass chamber sitting inside a set of two concentric coils, in turn sitting inside a set of three concentric layers of mu-metal. Careful demagnetization of the mu-metal in a 50 Hz AC field routinely gives a residual field of 10 to 30 nT inside this chamber. The field is controlled by a command voltage fed to a voltage controlled current amplifier. The set of coils are two concentric coils with the current running in opposite directions and balanced to give as close to zero field as possible on the outside. This is necessary to allow for the rapid change of the field inside the conductive mu-metal shields.

The chemical reaction is outlined in Fig. 6. An aqueous solution of hydroxyethyl acrylate, is hydrogenated by para-hydrogen in the presence of a soluble rhodium catalyst. The hydrogen is transferred without scrambling between molecules to the substrate to yield hydroxyethyl propionate. For spectroscopic experiments deuterium oxide was preferred whereas for imaging experiments, ordinary water was used as the solvent. Normally the experiments were run on a 5 ml scale involving 100 mg of hydroxyethyl acrylate. Immediately after field cycling, the reaction solution is transferred to either an NMR tube (spectroscopic experiments) or a syringe (imaging experiments). The NMR spectrometer used in the spectroscopic experiments, a Varian INOVA300 console, is equipped with an external trigger and set up to start the acquisition without delay. The time elapsed from field cycling to sampling of the spectrum is thereby kept to a minimum (about 7 s). The free induction decay in the spectroscopic experiment is aquired after applying a 4.0 μs pulse, corresponding to a flip angle of 30°. After determining chemical yield, the ^{13}C spectrum of the polarized product is referenced to a thermal spectrum of a ^{13}C labelled sample of known concentration, collected with the same parameter settings. This makes it possible to calculate the signal enhancement and the polarization of the reaction product.

The optimal ^{13}C polarization for hydroxyethyl propionate was obtained using a remagnetization time of 1.2 s. The observed decrease in polarization using longer remagnetization times we attribute to relaxation of the spin order of the two protons originating from para-hydrogen. The enhancement of the ^{13}C signal was $-37\,900$ compared with a thermal equilibrium signal at 7 T and 333 K. This corresponds to a polarization equal to -21%. As can be seen in Fig. 7 the polarization was negative, which was expected from simulations. The discrepancy between the experimentally obtained polarization and the theoretical polarization corrected for by ^{13}C relaxation (-25%), is most probably due to proton relaxation during field cycling. The longitudinal relaxation time for the carbonyl group ^{13}C was found to be 60 s at 7 T and 333 K.

For the in vivo experiment ^{13}C labeled material was used. In Fig. 8 we see a ^{13}C angiogram showing the head and neck part of a guinea pig. The pulse sequence used for data collection was the true FISP sequence [15]. The image was acquired in 230 ms.

7. Discussion

We have shown that a transfer of populations between energy levels following hydrogenation with para-hydrogen can be achieved by a diabatic–adiabatic field cycling scheme and that this yields a net polarization of ^{13}C. Theory indicates that there is an equal and opposing positive polarization of the protons, so the net polarization of the whole molecule is still zero, just as in para-hydrogen. It is, however, interesting to note that since the gyromagnetic ratio of proton and ^{13}C are different, the molecules now have a net magnetization.

The technique described in this work makes it feasable to produce a solution of molecules with strongly polarized ^{13}C spins that can be used as an imaging agent for magnetic resonance imaging. This enables rapid angiographic imaging, with an excellent contrast, since there is virtually no background signal. The main requirement for this method to work, in the context of MRI, is that the longitudinal relaxation time of the hyperpolarized spins is longer than or comparable to the time interval between field cycling and imaging. This requirement could also be fulfilled for molecules containing other nuclei than ^{13}C, one of the best candidates being ^{15}N.

References

[1] C.R. Bowers, D.P. Weitekamp, Transformation of symmetrization order to nuclear-spin magnetization by chemical reaction and nuclear magnetic resonance, Phys. Rev. Lett. 57 (1986) 2645–2648.

[2] C.R. Bowers, D.P. Weitekamp, Parahydrogen and synthesis allow dramatically enhanced nuclear alignment, J. Am. Chem. Soc. 109 (1987) 5541–5542.

[3] M.G. Pravica, D.P. Weitekamp, Net NMR alignment by adiabatic transport of parahydrogen addition products to high magnetic field, Chem. Phys. Lett. 145 (4) (1988) 255–258.

[4] G. Buntkowsky, J. Bargon, H.-H. Limbach, A dynamic model of reaction pathway effects on parahydrogen-induced nuclear spin polarization, J. Am. Chem. Soc. 118 (1996) 8677–8683.

[5] T.C. Eisenschmid, J. McDonald, R. Eisenberg, INEPT in a chemical way. Polarization transfer from parahydrogen to ^{31}P by oxidative addition and dipolar relaxation, J. Am. Chem. Soc. 111 (1989) 7267–7269.
[6] R. Eisenberg, T.C. Eisenschmid, M.S. Chinn, R.U. Kirss, Parahydrogen-induced polarization and polarization transfer in hydrogenation and oxidative addition reactions, Adv. Chem. 230 (1992) 47–74.
[7] J. Barkemeyer, M. Haake, J. Bargon, Hetero-NMR enhancement via parahydrogen labeling, J. Am. Chem. Soc. 117 (1995) 2927–2928.
[8] J. Natterer, O. Schedletzky, J. Barkemeyer, J. Bargon, S.J. Glaser, Investigating catalytic processes with parahydrogen: evolution of zero-quantum coherence in AA′X spin systems, J. Magn. Reson. 133 (1998) 92–97.
[9] J. Barkemeyer, J. Bargon, H. Sengstschmid, R. Freeman, Heteronuclear polarization transfer using selective pulses during hydrogenation with parahydrogen, J. Magn. Reson. Ser. A 120 (1996) 129–132.
[10] M. Haake, J. Natterer, J. Bargon, Efficient NMR pulse sequence to transfer the parahydrogen-induced polarization to hetero nuclei, J. Am. Chem. Soc. 118 (1996) 8688–8691.
[11] K. Golman, O. Axelsson, H. Jóhannesson, S. Månsson, C. Olofsson, J.S. Petersson, Parahydrogen-induced polarization in imaging: subsecond ^{13}C angiography, Magn. Reson. Med. 46 (2001) 1–5.
[12] C.R. Bowers, Sensitivity enhancement utilizing parahydrogen, in: D.M. Grant, R.K. Harris (Eds.), Encyclopedia of Nuclear Magnetic Resonance, vol. 9, Wiley, Chichester, 2002.
[13] L.D. Landau, E.M. Lifshitz, in: Quantum Mechanics (Non-Relativistic Theory) Course of Theoretical Physics, vol. 3, third ed., Butterworth–Heinemann, Oxford, 1998.
[14] D.A. McQuarrie, Statistical Mechanics, Harper Collins, New York, 1976.
[15] A. Oppelt, R. Graumann, H. Barfuss, H. Fischer, W. Hartl, W. Schajor, FISP-a new fast MRI sequence, Electromedica 54 (1986) 15–18.